Available online at www.sciencedirect.com
SCIENCE DIRECT®
Journal of Sound and Vibration 287 (2005) 383–394
JOURNAL OF SOUND AND VIBRATION
www.elsevier.com/locate/jsvi

Short Communication

Waves on fluid-loaded shells and their resonance frequency spectrum

X.L. Bao[a], H. Überall[a,*], P.K. Raju[b], A.C. Ahyi[b], I.K. Bjørnø[c], L. Bjørnø[c]

[a]*Physics Department, Catholic University of America, Washington, DC 20064, USA*
[b]*Department of Mechanical Engineering, Auburn University, Auburn, AL 36849-5341, USA*
[c]*Department of Industrial Acoustics, Technical University of Denmark, DK-2800 Lyngby, Denmark*

Received 3 March 2004; received in revised form 24 November 2004; accepted 14 December 2004

Abstract

Technical requirements for elastic (metal) cylindrical shells include the knowledge of their natural frequency spectrum. These shells may be empty and fluid-immersed, or fluid-filled in an ambient medium of air, or doubly fluid-loaded inside and out. They may support circumferential waves, or axially propagating waves both in the shell material, and in the fluid loading. Previous results by Bao et al. (J. Acoust. Soc. Am. 105 (1999) 2704) were obtained for the circumferential-wave dispersion curves on doubly loaded aluminum shells; the present study extends this to fluid-filled shells in air. For practical applications, steel shells are most important and we have here obtained corresponding results for these. To find the natural frequencies of cylindrical shells, one may invoke the principle of phase matching where resonating standing waves are formed around the circumference, or in the axial direction if the cylindrical shell is terminated at both ends. In this way, we obtain (circumferential and axial wave) eigenfrequency spectra for water filled aluminum and steel shells, and also for brass shells (axial-wave resonances only).

1. Introduction

The phase–velocity dispersion curves (plotted vs. frequency) of circumferentially propagating waves that encircle thin cylindrical (or spherical) metal shells are closely similar to those on a flat plate, see Refs. [1,2]. The prime example of the latter are the results of Schoch for a free plate,

*Corresponding author. Fax: +1-512-244 0944/+1-202-319 4448.

0022-460X/$ - see front matter © 2005 Elsevier Ltd. All rights reserved.
doi:10.1016/j.jsv.2004.12.006

reproduced in the first edition of the book by Brekhovskikh [3]. They show curves for symmetric (S_n) and antisymmetric (A_n) "Lamb waves", of which the higher ones ($n \geqslant 1$) have low-frequency cutoffs at which the curves tend to infinity. If the plates or shells are singly (or doubly) fluid loaded, one (or two) additional "Scholte–Stoneley waves" are added which can interact with the A_0-wave curve. Previous results were obtained for the case of aluminum plates, see Refs. [4,5], and cylindrical shells [6], demonstrating the effects of double fluid loading for the case of two different loading fluids with comparable densities. In the present study, intended for possible practical applications e.g. for a cylindrical pipe carrying a fluid flow, we obtain circumferential-wave dispersion curves for water-filled cylindrical shells (aluminum and steel) in air which do not appear in the previous literature. The eigenfrequency spectrum corresponding to these waves is found from their resonances that occur when they form standing waves around the circumference, based on the principle of phase matching [7]. This corresponds to a formation of standing waves around the shell's circumference, which can also be viewed as repeated encirclements (in both directions) of the shell where an integer number of wavelengths spans the circumference of the shell. This leads to a resonant reinforcement of the dispersive encircling waves (attenuated due to radiation into the loading fluid) at all those frequencies where the phase matching condition is satisfied, constituting the eigenfrequency spectrum of the shell.

In the following, we shall first obtain the phase–velocity dispersion curves of circumferential waves on water-filled aluminum and steel shells in air, and then the corresponding eigenfrequency spectrum as found from the phase matching condition. This is extended to the case of doubly fluid loaded aluminum shells, and in a subsequent section we obtain eigenfrequency spectra of axially propagating waves on shells terminated at both ends. Their spectra can be substantially different from those of the circumferential-wave spectra depending on the aspect ratio of the finite shell.

2. Circumferential-wave dispersion curves for fluid-filled shells

Phase–velocity dispersion curves of circumferential waves on fluid-filled cylindrical shells in air (or vacuum) have not been found in the literature (for brass shells, axial-wave dispersion curves only are available [8]). Below, we show the low-order circumferential-wave phase velocity (c_p) dispersion curves for water-filled aluminum and steel shells in air, obtained by the methods of Bao et al. [6]. We plot c_p/c_0 (normalized by the sound velocity in air, $c_0 = 340\,\mathrm{m/s}$) vs. the frequency variable $ka \equiv \omega a/c_0$, or alternately vs. $k_w a \equiv \omega a/c_w$ where $\omega = 2\pi f$ = circular frequency, a is the outer radius of the shell, and $c_w = 1483\,\mathrm{m/s}$ is the sound velocity in water (density $\rho_w = 1.0\,\mathrm{g/cm^3}$).

Fig. 1 shows the dispersion curves for a water-filled aluminum shell in air. The bulk wave velocities in aluminum are $c_L = 6350\,\mathrm{m/s}$ (compressional) and $c_T = 3050\,\mathrm{m/s}$ (shear waves), the density is $\rho = 2.7\,\mathrm{g/cm^3}$ and the density of air is $\rho_0 = 0.00129\,\mathrm{g/cm^3}$. The thickness parameter b/a (ratio of inner to outer radius) is 0.92.

Figs. 2 and 3 show corresponding curves for water-filled steel shells in air, for several kinds of steels and thicknesses. Figs. 2(a) and (b) correspond to steel shells of thickness $b/a = 0.963$ for steel types AISL 304L (Fig. 2(a)) and AISL 316L (Fig. 2(b)) with the following material parameters: AISL 304L has Young's modulus $E = 200\,\mathrm{kN/mm^2}$, Coulomb's modulus $G = 76.9\,\mathrm{kN/mm^2}$ and Poisson's ratio (at 20 °C, static) $\sigma = 0.245$; AISL 316L has $E = 195\,\mathrm{kN/mm^2}$,

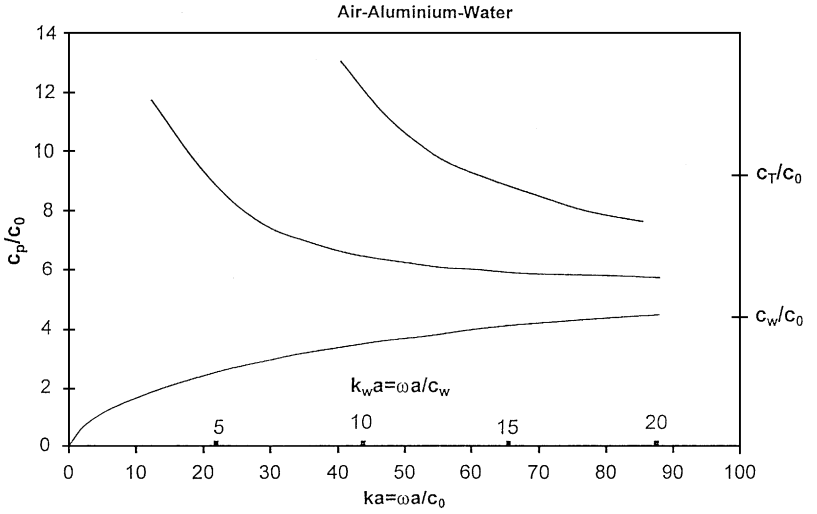

Fig. 1. Circumferential-wave phase velocity dispersion curves of an 8%-thick, water-filled cylindrical aluminum shell in air.

$G = 74\,\mathrm{kN/mm^2}$ and $\sigma = 0.255$. At a steel density of $\rho = 7.8\,\mathrm{g/cm^3}$, this leads to $c_L = 5521\,\mathrm{m/s}$ and $c_T = 3140\,\mathrm{m/s}$ for AISL 304L, and to $c_L = 5503\,\mathrm{m/s}$ and $c_T = 3080\,\mathrm{m/s}$ for AISL 316L, using the conversion formulas ([9,10])

$$c_L = [(E/\rho)(1-\sigma)/(1+\sigma)(1-2\sigma)]^{1/2}, \tag{1a}$$

$$c_T = (G/\rho)^{1/2}. \tag{1b}$$

It is seen that the dispersion curves for the two steel types differ only insignificantly and only at the higher-frequency values.

Figs. 3(a) and (b) correspond to a different type of steel, with $c_L = 5950\,\mathrm{m/s}$, $c_T = 3240\,\mathrm{m/s}$ and $\rho = 7.8\,\mathrm{g/cm^2}$, and with the thickness $b/a = 0.92$ (Fig. 3(a)) and $b/a = 0.88$ (Fig. 3(b)). Here, differences with Figs. 2, as well as between Figs. 3(a) and (b), are evident.

In all the preceding figures, which concern water-filled metal shells in air, the dispersion curves are seen to attain asymptotically at high frequencies the sound speed value in water, i.e. in the filling fluid. This shows them to be waves propagating in the filling fluid, in view of the fact that for both of our previously considered examples of an evacuated, water-immersed aluminum shell [6] and (exploiting the plate-shell similarity) for an aluminum plate loaded with water on one side and bounded by a vacuum on the other side [4,5], the phase–velocity dispersion curve tended towards the sound speed in the loading fluid (c_w) if the wave was fluid-borne, and towards the bulk-wave value c_T (or, for the lowest Lamb wave curves A_0 and S_0, towards the Rayleigh-wave speed c_R) in the metal if the wave was shell-(or plate-) borne. Apparently, thus, for a fluid-filled thin shell the circumferential wave modes propagating in the filler fluid show a certain predominance. Again, similarly to the Lamb waves, their lowest-mode phase velocity curve tends to zero at vanishing frequency (see, however, below), while those of the higher modes tend to infinity at certain low-frequency cutoffs. This behavior appears characteristic for very thin metal

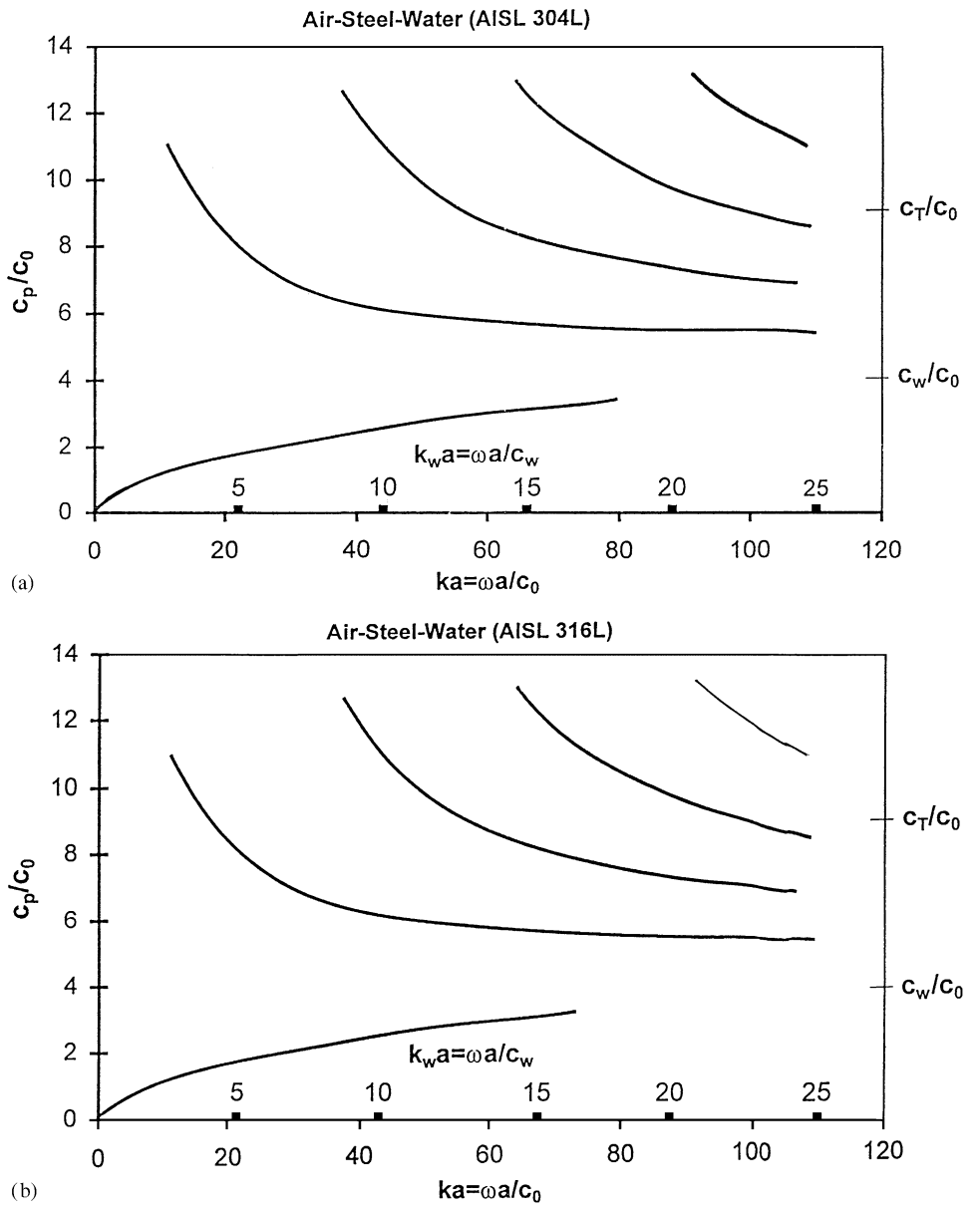

Fig. 2. (a) Circumferential-wave phase velocity dispersion curves of a 3.7%-thick, water-filled cylindrical AISL 304L steel shell in air. (b) Similarly for an AISL 316L steel shell.

shells in air (or vacuum) when filled with a liquid of substantial density (here, water); consider that the weight ratio of a steel shell with thickness $b/a = 0.963$ to the weight of the filler fluid (water) is 0.577, and of an aluminum shell with $b/a = 0.92$, it is 0.274.

The situation is comparable, as shown by us earlier [6] if the shell is loaded both inside and outside with fluids of substantial densities, e.g. Fig. 7 of Ref. [6] for a water-immersed,

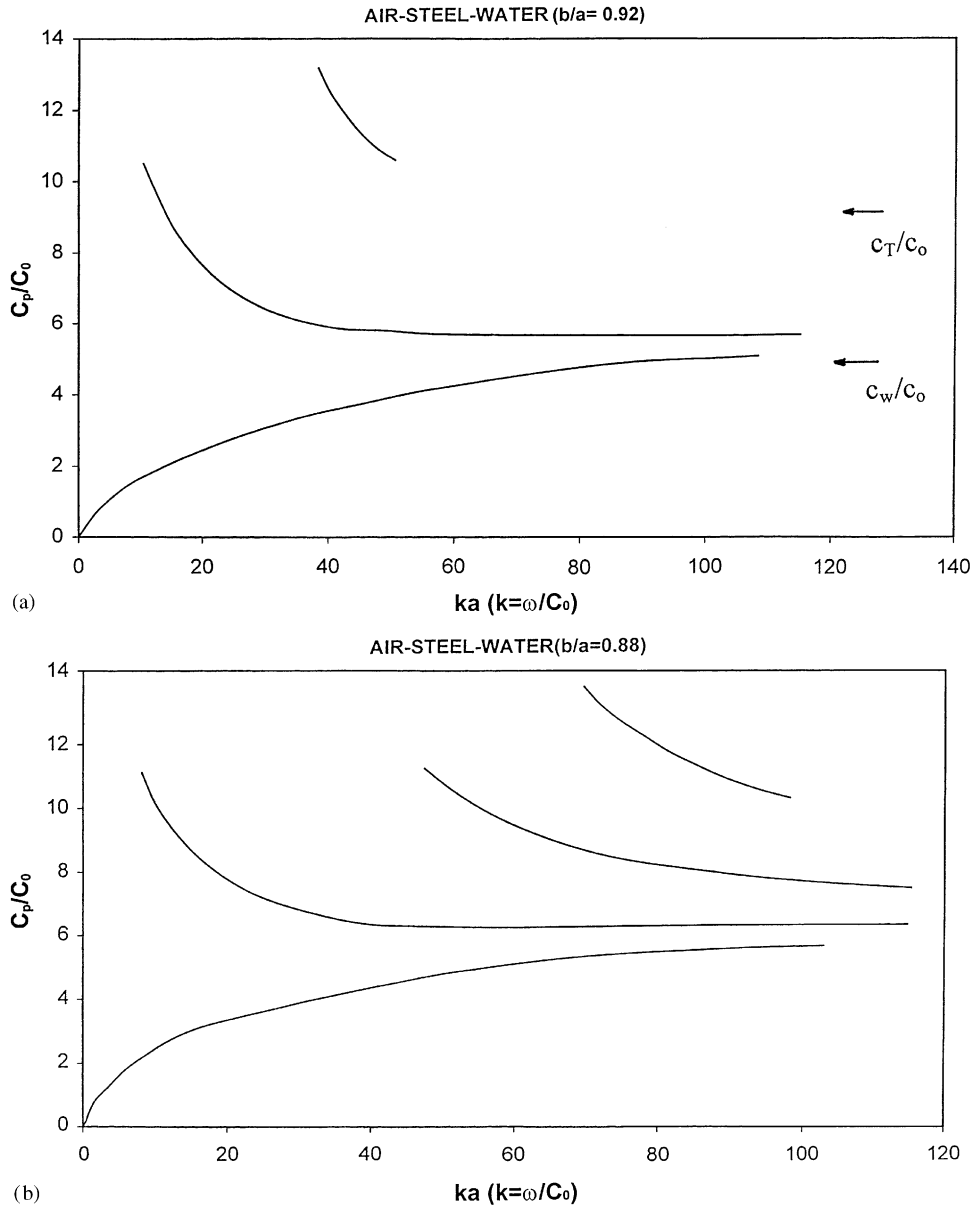

Fig. 3. (a) Circumferential-wave phase velocity dispersion curves of an 8% thick, water-filled cylindrical steel shell (parameters listed in the text) in air. (b) Similarly for a 12%-thick steel shell.

alcohol-filled aluminum shell with $b/a = 0.92$. Fig. 4 reproduces this figure from Ref. [6] for our subsequent use (the alcohol parameters, which inadvertently were not quoted in this reference, are $c_a = 1200\,\mathrm{m/s}$ and $\rho_a = 0.8\,\mathrm{g/cm^3}$). It was argued there that the lowest-order curve which tends to zero at vanishing frequency (as in Fig. 1) is a shell-borne wave at $k_w a \leqslant 15-20$ while a large number of descending higher-order mode curves $F_1, F_2, F_3 \ldots$ (as in the present case) all

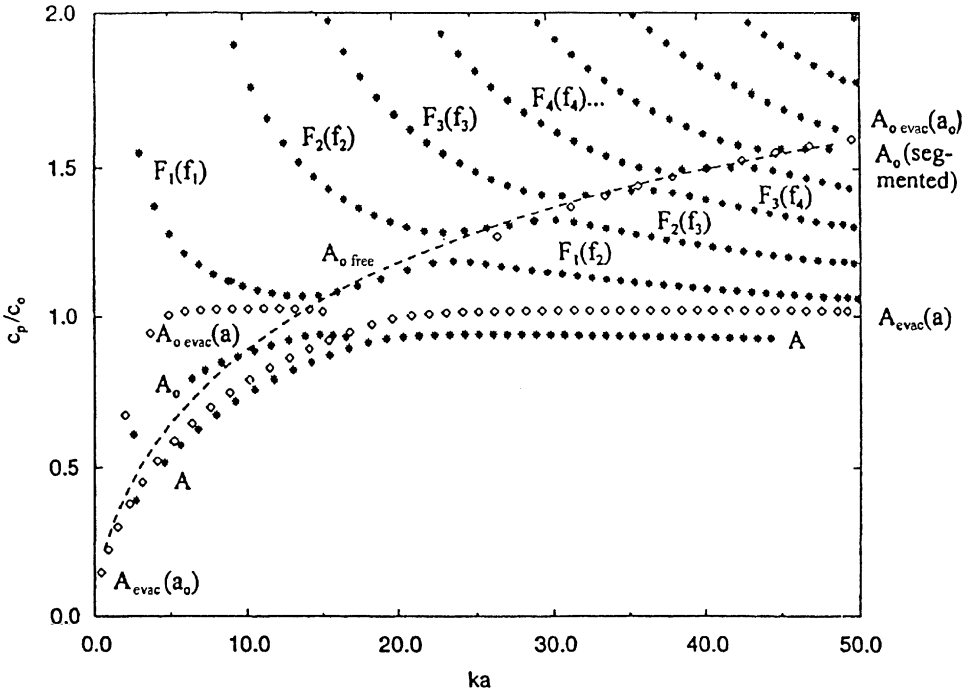

Fig. 4. Circumferential-wave phase velocity dispersion curves on an 8%-thick, water-immersed and alcohol-filled cylindrical aluminum shell. From Ref. [6].

correspond to waves in the filler fluid. Above $k_w a \geqslant 20$ it is seen that due to the compressional-shear coupling of the boundary conditions on the shell surface, these filler-fluid-borne mode curves successively approach each other (compare also Figs. 8 and 7 of Bao et al. [6]) and undergo curve repulsions [11] that leads to their systematic upward shifts by one unit. In the present case of Figs. 1–3, the curves do not reach much beyond $k_w a \sim 20$ so that one cannot tell from our data where, and to what extent, this repulsion phenomenon takes place here at higher values of $k_w a$. It may well be modified as compared to the case of double fluid loading [6].

3. Circumferential-wave eigenfrequency spectrum for fluid-filled shells

Practical applications often require a knowledge of the eigenfrequency spectrum of fluid-filled cylindrical metal shells. The eigenfrequencies corresponding to circumferential waves can be obtained from the above-given dispersion curves by using the principle of phase matching [7], in which a circumferential wave closes into itself with the same phase after each circumnavigation of a cylinder or cylindrical shell, leading to the formation of standing waves and hence resonant eigenfrequencies. The condition for phase matching, i.e. n wavelengths spanning the circumference, is $2\pi a = n\lambda$ (for a thin shell), or

$$c_p/c_0 = ka/n = (2\pi a/nc_0)f \tag{2}$$

Table 1
Circumferential-wave eigenfrequencies f_ℓ (in kHz) of water-filled cylindrical aluminum shell in air (shell radius $a = 5$ cm) corresponding to the three waves in Fig. 1 labeled $\ell = 1, 2, 3$ (from below)

n	$f(1)$	$f(2)$	$f(3)$
1	—	12.7	
2	—	20.5	
3	0.93	26.6	42.9
4	4.92	32.4	48.6
5	7.69	38.2	56.1

Table 2
Circumferential-wave eigenfrequencies f_ℓ (in kHz) of water-filled cylindrical AISL 304L—steel shell in air (shell radius $a = 5.4$ cm) corresponding to the waves in Fig. 2a labeled $\ell = 1, 2, 3, 4$ (from below)

n	$f(2)$	$f(3)$	$f(4)$
1	11.11		
2	17.89		
3	23.24	38.13	
4	28.21	44.34	
5	33.27	49.91	64.74

(where $k \equiv \omega/c_0$ is the wavenumber in the air). This equation represents a straight-line plot of c_p/c_0 vs. ka, and its intersections with the dispersion curves of Figs. 1–3 furnish the portion of the eigenfrequency spectrum of the fluid-filled cylindrical shell corresponding to the circumferential waves. Table 1 lists the eigenfrequencies of the water-filled cylindrical aluminum shell corresponding to Fig. 1, obtained in this way, and Table 2 those of the AISL 304L steel shell of Fig. 2(a). The graph of Fig. 5 shows the straight lines of Eq. (2) intersecting with the dispersion curves of Fig. 1, indicating how the entries of Table 1 were found. For completeness, we also list in Table 3 the values obtained from Fig. 4 for the eigenfrequencies of the alcohol-filled, water-immersed aluminum shell with $b/a = 0.92$.

4. Eigenfrequencies corresponding to axial standing waves

If the cylindrical shell is not infinitely long as assumed before, but is terminated at both ends and has a length L, then the phase matching condition for axially propagating waves (furnishing the resonant eigenfrequencies) leads to the formation of standing waves (assuming fixed terminations):

$$L = n\lambda/2, \quad n = 1, 2, 3 \ldots \tag{3a}$$

or

$$c_p/c_w = (k_w d/n)(L/\pi d) = (2L/nc_w)f \tag{3b}$$

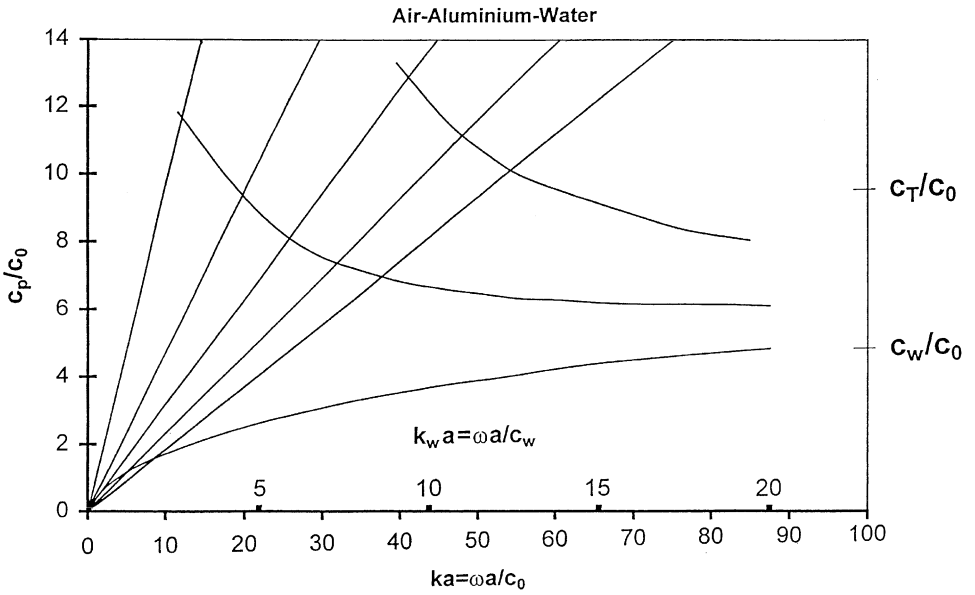

Fig. 5. Intersection of Eq. (2) with the dispersion curves of Fig. 1, furnishing the eigenfrequencies of a cylindrical water-filled aluminum shell (Table 1) due to the phase matching of circumferential waves.

Table 3
Circumferential-wave eigenfrequencies f_n (in kHz) of the alcohol-filled, water-immersed aluminum shell ($b/a = 0.92$, shell radius $a = 5$ cm) corresponding to the waves A, A_0, F_1, F_2, F_3 of Fig. 4

n	A	A_0	F_1	F_2	F_3
2			14.65		
3			19.88		
4		11.38	24.26		
5		15.41	28.82	45.01	
6		19.51	33.38	50.08	
7	13.13	24.55	37.85	55.01	
8	18.10	29.91	42.26	60.02	75.02

(where k_w is the wavenumber in the water filling, and we shall here use $k_w d$ as the frequency variable). This equation represents a straight-line plot of c_p/c_w vs. $k_w d$, and its intersection with the dispersion curves of axially propagating waves again furnishes a portion of the eigenfrequency spectrum of the fluid-filled cylindrical shell corresponding to the axially propagating waves. For aluminum and steel, these dispersion curves have not been found in the literature regarding fluid-filled cylindrical shells, but it may be sufficient to use here the dispersion curves on plates fluid-loaded on one side (aluminum: see Refs. [4–5,12]; steel: Ref. [12]) since for axially propagating waves, the transverse curvature of a cylindrical object is of little influence on the dispersion [13,14]. These curves (restricted to the A_0 wave and the Scholte–Stoneley wave A) are shown [12] in Fig. 6(a) for the one-sidedly water-loaded aluminum plate, and in Fig. 6(b) for the water-loaded

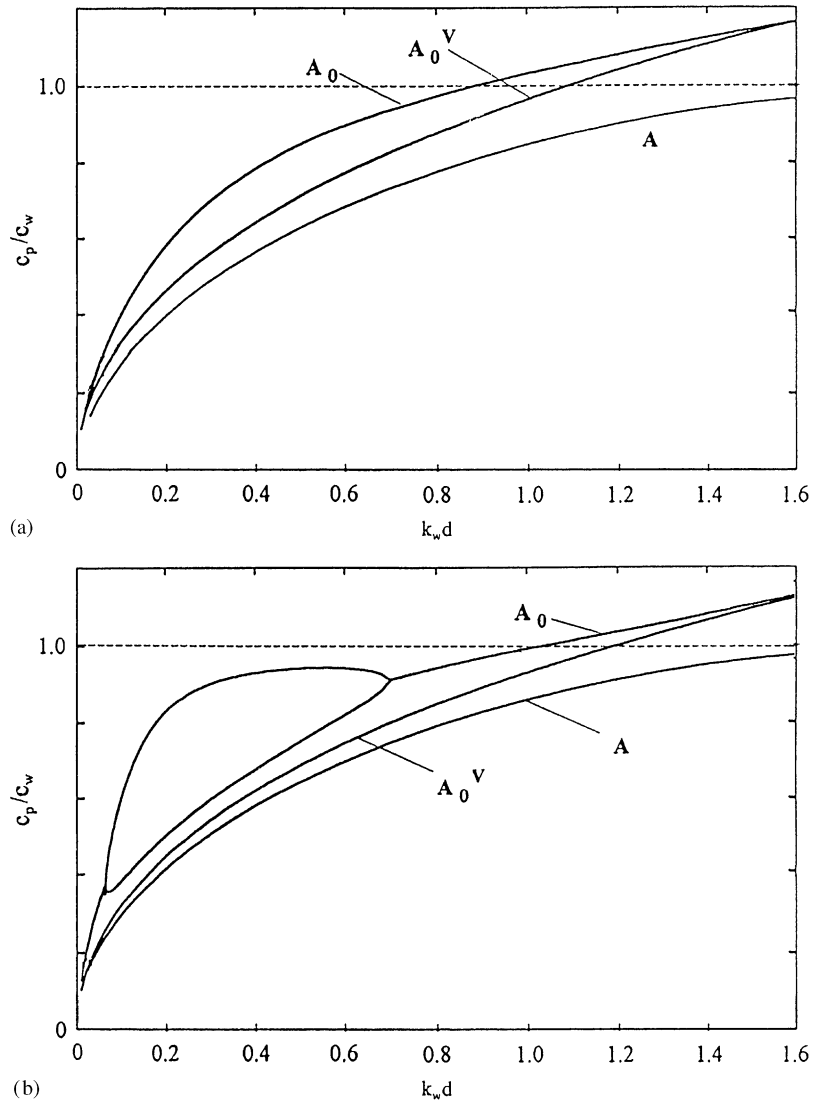

Fig. 6. (a) Dispersion curves of A_0 and A waves on aluminum plate with one-sided water loading (d = plate thickness). A_0^V refers to a plate in vacuum. (b) Similarly for a steel plate. From Ref. [12].

steel plate. Intersection with Eq. (3b) leads to the eigenfrequencies shown in Table 4 for an aluminum shell of length $L = 960\,\text{mm}$, and a steel shell of the same length (Table 5). The intersection with the higher-lying S_0 wave dispersion curve (see, e.g., Fig. 1 of Ref. [11], or Fig. 9 of Ref. [5]) leads to the much higher-lying eigenfrequencies for an aluminum plate, Table 6.

For the case of brass, the literature contains results by Kumar [8] on the dispersion curves of longitudinally propagating, axially symmetric waves on a water-filled cylindrical brass shell in vacuum. The material parameters for brass are [8] $c_L = 4.7 \times 10^5\,\text{cm/s}$, $c_T = 2.11 \times 10^5\,\text{cm/s}$, $\rho = 8.5\,\text{g/cm}^3$. In Fig. 7, we show dispersion curves of longitudinally propagating flexural waves,

Table 4
Eigenfrequencies f_ℓ (in kHz) of A_0 and A standing waves in the longitudinal direction on a water-filled aluminum shell in vacuum, of length 960 mm (fixed end pieces), outer radius $a = 5$ cm and wall thickness 4 mm, corresponding to Fig. 6a, or Fig. 1a of Ref. [12]

n	A_0	A
10	1.83	
20	7.5	3.35
30	15.8	8.1
40	25.6	14.1
50	34.7	21.5

Table 5
Eigenfrequencies f_ℓ (in kHz) of A_0 and A standing waves (including the duplication A_0' of the A_0 wave) in the longitudinal direction on a water-filled steel shell in vacuum of length 960 mm (fixed end pieces), outer radius $a = 5$ cm and wall thickness 4 mm, corresponding to Figs. 6b or 1b of Ref. [12]

n	A_0	A_0'	A
5	1.21		
10	2.78	—	1.77
20	13.0	6.52	3.96
30	21.2	12.3	8.85
40	28.8	20.1	14.9
50	36.0	30.3	22.8
60	43.1	—	31.6

Table 6
Eigenfrequencies f_ℓ (in kHz) of S_0 standing waves in the longitudinal direction on a water-filled aluminum shell in vacuum, of length 960 mm (fixed end pieces), outer radius $a = 5$ cm and wall thickness 4 mm, corresponding to Fig. 1 of Ref. [11]

n	S_0
1	2.85
2	5.69
3	8.52
5	14.21
10	28.41
20	56.82
30	85.19
40	113.58
50	141.90

extracted from Kumar's results and presented in the form of our preceding graphs, for a water-filled cylindrical brass shell of thickness $b/a = 0.9$ (Fig. 11 of Ref. [8]). This graph reaches to higher frequencies than our preceding new plots, and thus shows similar curve repulsion effects as

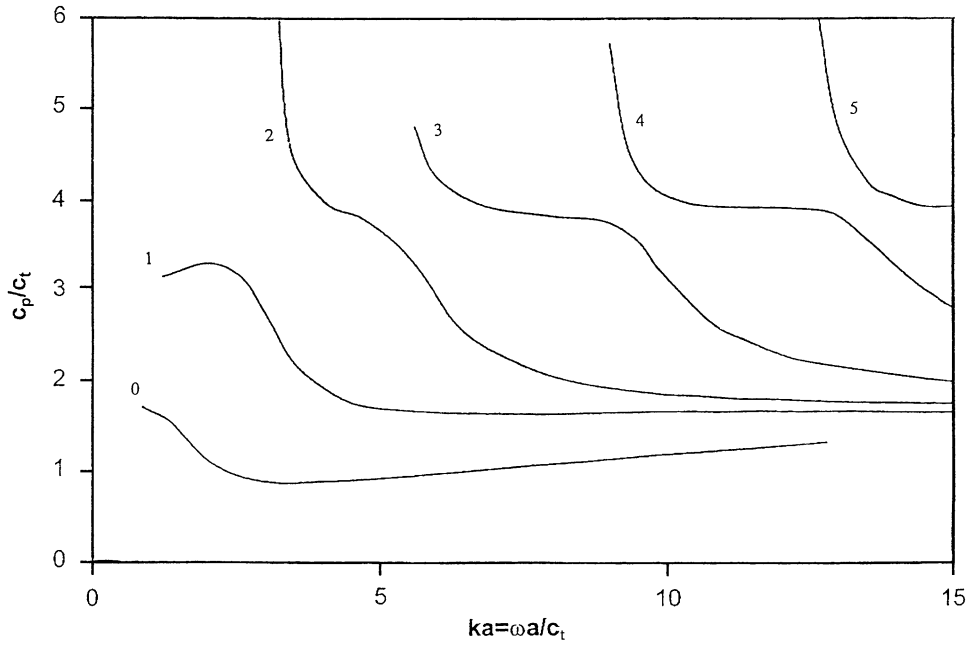

Fig. 7. Dispersion curves of c_p/c_T for flexural waves propagating longitudinally in a 10% thick water-filled cylindrical brass shell in vacuum. Adapted from Fig. 11 of Ref. [8].

Table 7
Eigenfrequencies f_ℓ (in kHz) of standing waves in the longitudinal direction on a water-filled brass shell in vacuum, of length 960 mm (fixed end pieces), outer radius $a = 5$ cm and $b/a = 0.9$, corresponding to Fig. 7 (adapted from Fig. 11 of Ref. [8])

n	$f(0)$	$f(1)$	$f(2)$	$f(3)$	$f(4)$
3	5.81	10.6	—	—	—
4	7.32	14.6	22.1		
5	8.74	17.3	24.0	—	—
6	9.59	19.0	26.6		
7	10.6	20.5	30.0	37.2	
8	11.6	21.7	33.0	39.1	
9	12.4	22.7	35.1	41.4	60.0
10	12.9	23.8	37.2	44.3	60.6

in Fig. 4 for the circumferential waves, which were not visible in our low-frequency curves of Figs. 1–3. Intersection of Eq. (3b) with the dispersion curves of Fig. 7 then furnishes the eigenfrequencies of the brass shell shown in Table 7, due to longitudinal standing waves of axial symmetry.

5. Summary

Cylindrical metal shells appear as part of countless items of industrial equipment. Nuclear, marine, petrochemical and many other industries employ cylindrical shells as conduits for fluid flow, and the knowledge of the vibrational characteristics of such shells (especially of their resonant eigenfrequencies) is a topic of primary importance. In the present study, obtaining the eigenfrequency spectrum of fluid-filled metal shells is shown to be facilitated by the knowledge of the dispersion curves of the waves propagating on these shells in either the circumferential or the longitudinal directions. In the course of this study, several new results for circumferential-wave dispersion curves of fluid-filled metal cylinders have been obtained. Application of the principle of phase matching, i.e. the formation of standing waves, then furnishes the eigenfrequency spectrum of the shell due to these waves. This is applied to water-filled aluminum, steel and brass shells, and it appears that for thin shells, a dominant role is played by the waves propagating in the fluid filling.

References

[1] H. Überall, A. Gérard, A. Guran, J. Duclos, M. El H. Khelil, X.L. Bao, P.K. Raju, Acoustic scattering resonances: relation to external and internal surface waves, *Applied Mechanics Reviews* 49 (1996) S63–S71.
[2] J.P. Sessarego, J. Sageloli, C. Gazanhes, H. Überall, Two-Scholte–Stoneley waves on doubly fluid-loaded plates and shells, *Journal of the Acoustical Society of America* 101 (1997) 135–142.
[3] L.M. Brekhovskikh, *Waves in Layered Media*, first ed, Academic Press, New York, 1960.
[4] X.L. Bao, H. Franklin, P.K. Raju, H. Überall, The splitting of dispersion curves for plates fluid-loaded on both sides, *Journal of the Acoustical Society of America* 102 (1997) 1246–1248.
[5] X.L. Bao, H. Franklin, P.K. Raju, H. Überall, O. Poncelet, Fluid-borne and Lamb-type waves on elastic plates in contact with two different fluids, *Acta Acustica* 84 (1998) 823–829.
[6] X.L. Bao, P.K. Raju, H. Überall, Circumferential waves on an immersed, fluid-filled elastic cylindrical shell, *Journal of the Acoustical Society of America* 105 (1999) 2704–2709.
[7] H. Überall, L.R. Dragonette, L. Flax, Relation between creeping waves and normal mode of vibration of a curved body, *Journal of the Acoustical Society of America* 61 (1977) 711–715.
[8] R. Kumar, Dispersion of axially symmetric waves in empty and fluid-filled cylindrical shells, *Acustica* 27 (1972) 317–329.
[9] A.M. Howatson, et al., *Engineering Tables and Data*, Chapman & Hall, Norwell, MA, 1972.
[10] W.P. Mason, Acoustic properties of solids, in: *American Institute of Physics Handbook*, McGraw Hill, New York, 1972.
[11] H. Überall, B. Hosten, M. Deschamps, A. Gérard, Repulsion of phase velocity dispersion curves and the nature of plate vibrations, *Journal of the Acoustical Society of America* 96 (1994) 908–917.
[12] J. Metsaveer, A. Klauson, Influence of the curvature on the dispersion curves of a submerged cylindrical shell, *Journal of the Acoustical Society of America* 100 (1996) 1551–1560.
[13] H. Hönl, A.W. Maue, K. Westpfahl, Theorie der Beugung, in: *Handbuch der Physik XXV/1, Kristalloptik-Beugung*, Springer, Berlin, 1956, pp. 218–591.
[14] W. Franz, K. Deppermann, Theorie der Beugung am Zylinder unter Berücksichtigung der Kriechwelle, *Annals of Physics* 10 (1952) 361–373.